

Robust Facial Expression Recognition with Convolutional Visual Transformers

Fuyan Ma, Bin Sun, *Member, IEEE*, and Shutao Li, *Fellow, IEEE*

Abstract—Facial Expression Recognition (FER) in the wild is extremely challenging due to occlusions, variant head poses, face deformation and motion blur under unconstrained conditions. Although substantial progresses have been made in automatic FER in the past few decades, previous studies are mainly designed for lab-controlled FER. Real-world occlusions, variant head poses and other issues definitely increase the difficulty of FER on account of these information-deficient regions and complex backgrounds. Different from previous pure CNNs based methods, we argue that it is feasible and practical to translate facial images into sequences of visual words and perform expression recognition from a global perspective. Therefore, we propose Convolutional Visual Transformers to tackle FER in the wild by two main steps. First, we propose an attentional selective fusion (ASF) for leveraging the feature maps generated by two-branch CNNs. The ASF captures discriminative information by fusing multiple features with global-local attention. The fused feature maps are then flattened and projected into sequences of visual words. Second, inspired by the success of Transformers in natural language processing, we propose to model relationships between these visual words with global self-attention. The proposed method are evaluated on three public in-the-wild facial expression datasets (RAF-DB, FERPlus and AffectNet). Under the same settings, extensive experiments demonstrate that our method shows superior performance over other methods, setting new state of the art on RAF-DB with 88.14%, FERPlus with 88.81% and AffectNet with 61.85%. We also conduct cross-dataset evaluation on CK+ show the generalization capability of the proposed method.

Index Terms—Facial expression recognition in the wild, global-local attention, Transformers, global self-attention.

1 INTRODUCTION

UNDERSTANDING human emotional states is the fundamental task to develop emotional intelligence, which is an interdisciplinary field spanning from different research areas, such as psychology and computer science. Facial expression is one of the most natural, powerful and universal signals for human beings to convey their emotional states and intentions [1], [2]. Facial expression recognition (FER) systems have various applications, including human-robot interaction (HRI), mental health assessment and driver fatigue monitoring. Therefore, numerous research endeavours have been invested for promoting the development of FER. With the advance of machine learning, especially deep learning, researchers have made great progress on FER in the past decades. Before deep learning era, traditional FER methods have mainly used handcrafted features and shallow learning (e.g., Histograms of Oriented Gradients (HOGs) [3], Local Binary Patterns (LBP) [4], [5], non-negative matrix factorization (NMF) [6] and sparse representation [7]). With the popularity of data-driven techniques, convolutional neural networks (CNNs) [8] based methods have exceeded traditional methods by a large margin and achieved state-of-the-art FER performance

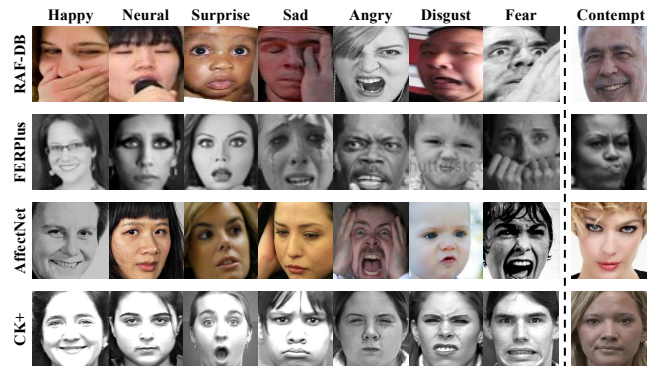


Fig. 1. Samples from RAF-DB, FERPlus, AffectNet and CK+. Variant head poses, occlusions and other unconstrained conditions can be seen in above examples. Note that RAF-DB is annotated with seven basic expressions and FERPlus, AffectNet, CK+ are with eight expression labels, including the contempt category.

(e.g., [9], [10], [11], [12]).

Despite the significant success of learned representation for constrained FER, the performance of FER in the wild is still far from satisfactory. Majority of these proposed algorithms are implemented on lab-collected datasets, such as CK+ [13], MMI [14] and Oulu-CASIA [15]. These algorithms perform perfectly on these lab-collected FER datasets, because the controlled images are frontal with minimal illumination changes and limited occlusions. However, the performance degrades dramatically on these real-world FER datasets, such as RAF-DB [9], FERPlus [16] and AffectNet [17]. Compared with the real-world FER datasets, the number of images from lab-collected FER datasets is relatively

• Fuyan Ma and Bin Sun are with College of Electrical and Information Engineering, and with the Key Laboratory of Visual Perception and Artificial Intelligence of Hunan Province, Hunan University, Changsha, 410082, China.(mafuyan@hnu.edu.cn; sunbin611@hnu.edu.cn).

• Shutao Li is with College of Electrical and Information Engineering, with the State Key Laboratory of Advanced Design and Manufacturing for Vehicle Body and with the Key Laboratory of Visual Perception and Artificial Intelligence of Hunan Province, Hunan University, Changsha, 410082, China.(shutao.li@hnu.edu.cn)

small. Especially, the CNNs for the FER in the wild usually require sufficient training face images to ensure generalizability for real applications. Most publicly available datasets for FER do not have a sufficient quantity of images for training. Therefore, the data augmentation approaches (i.e., on-the-fly data augmentation, offline data augmentation) are significantly important for the FER by deep learning techniques.

Different backgrounds, illuminations and head poses are fairly common in the wild, which are irrelevant to facial expressions [18]. Especially, directly recognizing expression on non-frontal faces caused by variant head poses is a big challenge [19]. To remove complex backgrounds and non-face areas, it is indispensable to detect faces before training the deep neural network to learn meaningful features. Several face detectors like MTCNN [20] and Dlib [21] are used to detect faces in complex scenes. The face alignment is also crucial because it can reduce the variation in facial size and in-plane rotation. After extracting facial features, the next stage is to feed the features into classifiers such as Support Vector Machines (SVMs) and the softmax layer. Unlike these traditional methods, the deep CNNs perform feature extraction and classification in an end-to-end manner, which has greatly improved representation capacity of learned features for facial expression recognition.

As shown in Fig. 1, the challenges of FER in the wild mainly come from occlusions, variant head poses, face deformation, motion blur, insufficient qualitative data, etc., which lead to significant change of facial appearance. These unexpected issues definitely increase the difficulty of FER in the wild. In order to tackle these problems, various methods have been proposed to improve the FER accuracy and enhance the generalization ability of algorithms. Most of the researchers design their methods for occlusion-aware FER. Bourel et al., [22] proposed to recover facial feature points for the recognition of facial expressions in the presence of occlusion. Happy and Routray [23] present a framework for FER by using appearance features of salient facial patches and removing features of occlusion patches. Li et al., [24] proposed a patch-gated CNN that integrates path-level attention for expression recognition with occlusion. Besides, attention models have been successfully applied for FER to explore meaningful regions. Similar to [24], a series of methods, such as [11], [25], [26], also used attention-like mechanisms to focus on the most discriminative features to improve FER accuracy in the wild. Some researchers also aim at tackling multi-view facial expression recognition. In [27], Sun et al., proposed cyclic image generation for unsupervised cross-view facial expression based on generative adversarial networks. Zheng et al., [28] proposed a transductive transfer learning method for cross-domain color facial expression recognition. Facial images from source domain are combined with facial images from target domain to jointly learn a discriminative subspace, and an SVM classifier is trained for expression recognition. Zheng proposed a group sparse reduced-rank regression (GSRRR) model for multi-view facial expression recognition. Based on GSRRR, the whole model automatically selected the optimal sub-regions of a face that contribute most to the expression recognition.

Inspired by the interesting phenomenon that we can

understand the sentences in out-of-order or missing some words, we propose to recognize facial expressions globally based on sequences of visual words. Also like the image description task in Natural Language Processing (NLP), we may use several visual words to describe the emotional state for an image. Therefore, we propose Convolutional Visual Transformers (CVT) for robust facial expression recognition in the wild. Our method combines LBP features and CNN features to further enrich the representation of visual words, referring to the hybrid feature extraction. The reason we use LBP features is that it can catch the small movements of the faces and extract image texture information. We design an attentional feature fusion (ASF) to adaptively integrate LBP features and CNN features. The ASF aggregates both global and local relationships between two kinds of features, which can effectively improve the recognition performance. We simply convert the fused feature maps into a sequence of visual words by flattening and projecting the features maps. After obtaining these visual words, We then exploit the promising learning capabilities of multi-layer Transformer encoder to boost the performance. Global self-attention in multi-layer Transformer encoder allows the network to model contextual information of the representative visual words and focus on the most discriminative features.

Overall, the main contributions of our work can be summarized as follows:

- 1) We propose Convolutional Visual Transformers for FER in the wild, which integrates LBP features and CNN features with global-local attention and global self-attention for improving expression recognition accuracy.
- 2) We design a simple but effective feature fusion module named ASF to aggregate both global and local facial information. Moreover, ASF guides the backbones to extract the required information while squeeze the useless information in an end-to-end manner.
- 3) To the best of our knowledge, we are the first to apply Transformers for FER. Global self-attention enables the whole network to learn the relationships between elements of visual feature sequences, which ignores these information-deficient regions.
- 4) Extensive experimental results on three publicly available FER in the wild datasets, i.e., RAF-DB, FERPlus and AffectNet demonstrate that our CVT can achieve state-of-the-art expression recognition accuracies. Especially, we also conduct experiments on occlusion and variant pose subsets of these three datasets and cross-dataset evaluation on CK+ to show promising generalization ability of our method.

The rest of this article is organized as follows: Section II briefly reviews related works for FER in the wild and provides a comprehensive review of recent advances in FER. The core idea of our proposed CVT is presented in Section III. Section IV presents an extensive performance evaluation for the proposed method and state-of-the-art approaches. We conclude our work and give future work in Section V.

2 RELATED WORK

2.1 Facial Expression Recognition in the Wild

Facial expression recognition has been an emerging topic with the development of deep learning, especially convolutional neural networks. CNNs have shown promising results in FER on lab-collected datasets. However, the performance of FER in the wild is heavily influenced by unexpected conditions mentioned in Section 1. One critical step for FER in the wild is to accurately extract discriminative features. Researchers start to shift their attention from hand-crafted features to deep features for facial expression recognition. Various architectures have been proposed for extracting deep features, such as Deep Belief Networks, ResNet [29], DenseNet [30]. Tang [31] utilized CNNs for feature extraction and replaced softmax layer with linear SVMs, which gave significant gains and won the ICML 2013 Representation Learning Workshop’s face expression recognition challenge.

To recognize facial expressions in the wild, Li et al., [9] proposed to enhance the discriminative power of deep features by a deep locality-preserving CNN (DLP-CNN) method. Region-based attention networks are especially suitable for FER in the wild, because they allow for salient face features to dynamically come to forefront when some occlusions or clutters occur in an image. In [11], Wang et al., proposed region attention networks (RAN) to capture the importance of facial regions for occlusion and pose variant FER. Likewise, Li [10] et al., proposed a CNN with attention mechanism for Occlusion Aware FER, which focused on the most discriminative face regions. Some FER algorithms integrated demographic features (i.e., gender, race, age, etc.) for improving the expression recognition performance. It is worth mentioning that Fan [25] proposed a deeply-supervised attention network, which takes facial attributes into consideration. In addition, Xu et al., [32] conducted a comparative study of the bias and fairness for FER and use the attribute information as input to address bias. Wang et al., [12] proposed a self-cure Network (SCN) to suppress the uncertainties for FER in the wild. SCN also took full advantage of attention mechanism to weight each training face sample. To improve FER accuracy in the wild, we incorporate global-local attention to integrate both LBP features and CNN features to get informative visual words. We also apply global self-attention to model relationships between visual words, which allows for suppressing confusing regions and highlighting discriminative features.

2.2 Feature Fusion for FER

Multi-scale feature fusion in deep learning has been widely invested for a multitude of applications, such as face recognition [33], object detection [34], semantic segmentation [35]. However, deep learning based methods require huge amount of data to generalize well. Fusing different feature maps can enrich the representative ability of the whole networks, which can effectively improve the generalization ability and the recognition performance. As we mentioned in Section 1, there are various hand-crafted features, such as HOGs [36] and LBP [37], which have been well-developed for facial expression feature representation. Besides, CNNs have been proposed for FER in the wild due to the powerful

representation capability. Chen et al., [38] proposed to fuse dynamic textures, geometric features and acoustic features to tackle FER in the wild. The dynamic texture descriptor of visual information is an extension of HOGs, named Histogram of Oriented Gradients from Three Orthogonal Planes (HOG-TOP). Shao and Qian [39] proposed a dual branch CNN to extracts LBP features and deep features parallel. Concatenation operation are then utilized to fuse these feature maps. Li et al., [26] combined LBP features and CNN features with dense connection to improve expression recognition accuracy. Previous feature fusion method often use element-wise summation or concatenation operation as fusion strategy. They don’t well utilize complementary information and abandon redundant information. Additionally, these feature fusion methods are mainly conducted on lab-controlled FER datasets, such as CK+ and Oulu-CASIA. Different from existing methods, we propose attentional selective fusion (ASF) for integrating LBP features and CNN features, which squeezes the useless information and generates correlated weight maps from both local and global perspectives. ASF is applied for FER datasets in the wild (RAF-DB, FERPlus and AffectNet), and the results in Table 5 prove the effectiveness of our ASF.

2.3 Transformers in Computer Vision

Transformers [40] have shown dominant performance in NLP. Inspired by the success of Transformers, several researchers have tried to invest Transformers on computer vision tasks, such as object detection [41], pose estimation [42], high-resolution image synthesis [43], video instance segmentation [44], trajectory prediction [45], etc. Vision Transformer (ViT) [46] is the first work to apply a vanilla Transformer to images with few modifications. ViT directly split an image into patches and fed these patches into a Transformer. According to [46], ViT yielded lower accuracy compared with ResNet when trained on ImageNet [47]. ViT was firstly trained on large datasets, and then fine-tuned for downstream tasks, because Transformers need amounts of data to generalize well on computer vision tasks. Wang et al., [48] proposed Pyramid Vision Transformer (PVT) for pixel-level dense prediction. PVT can work as the feature extraction backbone without convolutions, but with feature pyramid structure. Both ViT and PVT are pure Transformers without convolution operation. Transformer-based approaches have shown superior performance compared with CNN-based methods, when fully trained on large-scale datasets. Inspired by the vanilla Transformer and ViT, we firstly propose to directly apply Transformers for FER. Transformers model long dependencies between input sequences using global self-attention mechanism. Applying global self-attention for face images with occlusions or variant poses enables ignoring these information-deficient regions and recognizing expressions from a global perspective.

3 METHOD

In this section, we first elaborate the overview of the proposed Convolutional Visual Transformers for FER. Then, we explicitly illustrate the attentional selective fusion, and multi-Layer Transformer encoder in our whole network.

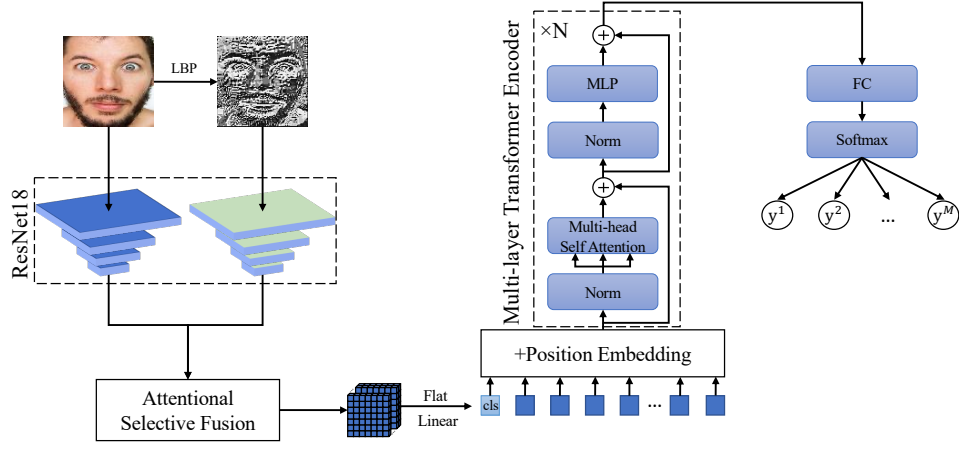


Fig. 2. An overview of our proposed Convolutional Visual Transformers. It can be divided into three parts, visual words extraction, relationship modeling and expression classification. pre-trained ResNet18 is used as the backbone to extract feature maps. All the extracted features are fused by our Attentional Selective Fusion to get representative visual words. The input visual words is obtained by simply flattening the spatial dimensions of the feature map and projecting to the specific dimension. And apply multi-layer Transformer encoder to model relationships between different visual features components. The network finally predicts expression by simple softmax function.

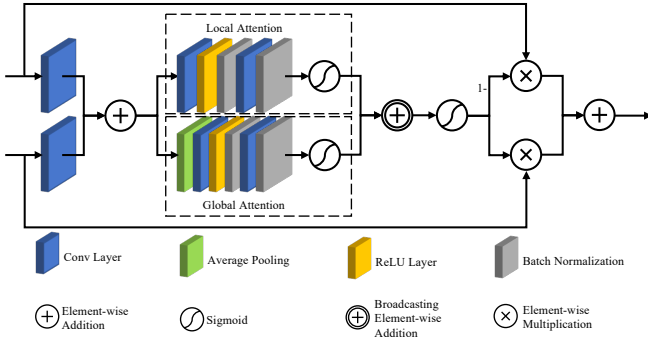


Fig. 3. Attentional Selective Fusion.

3.1 Overview

We illustrate the overall diagram of our Convolutional Visual Transformer for Facial Expression Recognition. Our CVT is built upon on two pre-trained ResNet18 [29] networks, and consists of two crucial components: i) attentional selective fusion, ii) multi-Layer Transformer encoder, as shown in Fig. 2.

For a given face image \mathbf{I}_{RGB} with the size of $H \times W \times 3$, we first get its LBP feature image $H \times W \times 1$ and concatenate it to a feature image \mathbf{I}_{LBP} with the size of $H \times W \times 3$. The feature extraction backbones are composed of two ResNet18 networks: one is for the raw image and the other is for its LBP feature image. Particularly, we employ the first five stages of ResNet18 as the backbone to extract feature maps \mathbf{X}_{LBP} and \mathbf{X}_{RGB} with the size of $\frac{H}{R} \times \frac{W}{R} \times C_f$, where R is the downsampling rate of ResNet18, C_f is the channel number of the output of the stage 5. For simplicity, we denote $H_d = \frac{H}{R}$ and $W_d = \frac{W}{R}$. In this paper, $R = 32$ and $H = W = 224$. We initialize the whole network weights by the pre-trained weights on MS-Celeb-1M face recognition dataset. Without loss of generalization, ASF is utilized to combine the features extracted from the raw image and the features extracted from its LBP feature image, which will be introduced in Section 3.2 in detail. The ASF works

by dynamically adjusting the weights of these features and guiding the networks focus more on discriminative features that are vital for improving expression recognition. The fusion weights of ASF are generated via global-local attention, which aggregates global and local context for further expression recognition. The size of fused feature maps \mathbf{F} is also $H_d \times W_d \times C_f$. Afterwards, we feed the flattened features to a linear projection and a learnable classification token is added. We get embedded visual words with size of $(H_d W_d + 1) \times C_p$, where C_p is the channel of flattened features after projection. We also add position embeddings to the embeddings to retain positional information, as [40] and [46] do. The input embeddings are further feed to the Transformer encoder, which is composed of N encoder blocks. The probabilities of facial expressions are generated by a fully connected layer and the softmax function.

3.2 Attentional Selective Fusion

Our attentional selective fusion consists of global attention and local attention, as can be seen in Fig. 3, which can provide additional flexibility in fusing different types of information. As mentioned in the Section 3.1, given two feature maps $\mathbf{X}_{LBP}, \mathbf{X}_{RGB} \in \mathbb{R}^{H_d \times W_d \times C_f}$ extracted from the backbones, we first fuse LBP features \mathbf{X}_{LBP} and CNN features \mathbf{X}_{RGB} for capturing subsequent information interaction:

$$\mathbf{U} = W_L \mathbf{X}_{LBP} + W_C \mathbf{X}_{RGB}, \quad (1)$$

where \mathbf{U} is the integrated feature maps after summation between \mathbf{X}_{LBP} and \mathbf{X}_{RGB} , and $+$ denotes element-wise summation. W_L and W_C are the weights for initial integration and simply implemented by two 1×1 convolutions. To perform both global and local selective fusion, we then choose global average pooling and the pixel-wise convolution as global context and local context aggregator, respectively. The global context and local context are computed as follows:

$$\mathbf{G}(\mathbf{U}) = \sigma(\text{BN}(\text{Conv}_G^2(\delta(\text{BN}(\text{Conv}_G^1(\text{AP}(\mathbf{U}))))))), \quad (2)$$

$$\mathbf{L}(\mathbf{U}) = \sigma(\text{BN}(\text{Conv}_L^2(\delta(\text{BN}(\text{Conv}_L^1(\mathbf{U})))))), \quad (3)$$

where $\mathbf{G}(\mathbf{U}) \in \mathbb{R}^{1 \times 1 \times C_f}$ and $\mathbf{L}(\mathbf{U}) \in \mathbb{R}^{H_d \times W_d \times 1}$ represent global fusion and local fusion weights. $\mathbb{A}\mathbb{P}$ denotes global adaptive average pooling, which is carried out using equation (4).

$$\mathbb{A}\mathbb{P}(\mathbf{U}) = \frac{1}{H_d W_d} \sum_{i=1}^{H_d} \sum_{j=1}^{W_d} x_c(i, j), c = 1, 2, \dots, C_f, \quad (4)$$

where H_d and W_d are the height and width of the input feature map \mathbf{U} , and C_f is the the number of channels of \mathbf{U} . $\mathbb{B}\mathbb{N}$ is the Batch Normalization. δ denotes the ReLU function, and σ denotes the Sigmoid function. The kernel sizes of Conv_G^1 and Conv_G^2 are $1 \times 1 \times C_f \times \frac{C_f}{r}$, $1 \times 1 \times \frac{C_f}{r} \times C_f$. We set r to 8 in this paper. Similarly, $L(\mathbf{U}) \in \mathbb{R}^{H_d \times W_d \times 1}$ is the local fusion weights. And the kernel sizes of Conv_L^1 , Conv_L^2 are $1 \times 1 \times C_f \times \frac{C_f}{r}$, $1 \times 1 \times \frac{C_f}{r} \times 1$. Given the global fusion weights $G(\mathbf{U})$ and the local fusion weights $L(\mathbf{U})$, the refined global-local attention weights can be obtained by (5).

$$\text{GL}(\mathbf{U}) = \mathbf{G}(\mathbf{U}) \oplus \mathbf{L}(\mathbf{U}), \quad (5)$$

where \oplus represents the broadcasting addition. Then, the fused feature map $\mathbf{X}_{\text{fused}}$ is calculated by as follows:

$$\begin{aligned} \mathbf{X}_{\text{fused}} = & \mathbf{X}_{\text{LBP}} \times \sigma(\text{GL}(\mathbf{U})) + \\ & \mathbf{X}_{\text{CNN}} \times \sigma(1 - \text{GL}(\mathbf{U})), \end{aligned} \quad (6)$$

where \times is the element-wise multiplication.

3.3 Multi-Layer Transformer Encoder

The fused 2D feature map $\mathbf{X}_{\text{fused}}$ need to be flattened into a 1D sequence, and further can be fed for the Transformer encoder as input. Therefore, we reshape $\mathbf{X}_{\text{fused}} \in \mathbb{R}^{H_d \times W_d \times C_f}$ into a flattened sequence and feed it to a linear projection to get $\mathbf{X}_f \in \mathbb{R}^{H_d W_d \times C_p}$, where $H_d W_d$ is the sequence length. As in [46], a classification token [cls] is appended at the beginning of the input sequence \mathbf{X}_f . The learnable state of the [cls] token at the output of the Transformer encoder is used to represent the whole feature sequence, which serves for the final prediction. To incorporate the position information in the multi-layer Transformer encoder, the 1D learnable positional embeddings are added to the feature embeddings:

$$\mathbf{Z}^0 = [\mathbf{x}_{\text{cls}}; \mathbf{x}_f^1; \mathbf{x}_f^2; \mathbf{x}_f^3; \dots; \mathbf{x}_f^{H_d W_d}] + \text{PE}(H_d W_d + 1; C_p), \quad (7)$$

where $\text{PE}(H_d W_d + 1; C_p) \in \mathbb{R}^{(H_d W_d + 1) \times C_p}$ learns the embeddings for each position index, [cls] token included. And \mathbf{Z}^0 represents the resulting position-aware feature sequence.

To model the complex interactions among all elements of the facial feature embeddings, we input \mathbf{Z}^0 to the standard multi-Layer Transformer encoder. The Transformer encoder calculates the weights of embeddings \mathbf{Z}^0 through multi-head self-attention (MHSA). This is done by learnable queries Q , keys K , and values V . We compute single-head global self-attention (SHSA) using Equation (8). Details of SHSA in the first layer can be formulated as follows:

$$\begin{aligned} \text{head}_j &= \text{Attention}(Q_j, K_j, V_j) \\ &= \text{softmax}\left(\frac{Q_j K_j^T}{\sqrt{d}}\right) V_j \\ &= \text{softmax}\left(\frac{Z^0 W_j^Q (Z^0 W_j^K)^T}{\sqrt{d}}\right) Z^0 W_j^V, \end{aligned} \quad (8)$$

where $Q_j = Z^0 W_j^Q$, $K_j = Z^0 W_j^K$, $V_j = Z^0 W_j^V$ and $W_j^Q \in \mathbb{R}^{C_p \times d}$, $W_j^K \in \mathbb{R}^{C_p \times d}$, $W_j^V \in \mathbb{R}^{C_p \times d}$ are parameters of linear projections. Specifically, multi queries, keys and values project Z^0 into N different representation subspaces. Multi-head self-attention (MHSA) can be described as:

$$\text{MHSA}(\mathbf{Z}^0) = \text{concat}(\text{head}_1, \dots, \text{head}_N) W^O, \quad (9)$$

where N is the number of different heads, and concat denotes the concatenation operation. $W^O \in \mathbb{R}^{h_1 \times d}$ are parameters of a linear projection, where the dimension of each head d is equal to $\frac{C_p}{N} = N$ and h_1 is the hidden size of the first layer. Each Transformer encoder consists of N layers of MHSA blocks. Formally, the standard multi-layer Transformer encoder computes forwardly for $i = 1, \dots, N$ layers:

$$\hat{\mathbf{Z}}^i = \text{MHSA}(\text{LN}(\mathbf{Z}^{i-1})) + \mathbf{Z}^{i-1} \quad (10)$$

$$\mathbf{Z}^i = \text{MLP}(\text{LN}(\hat{\mathbf{Z}}^i)) + \hat{\mathbf{Z}}^i \quad (11)$$

$$\mathbf{Y} = \text{LN}(\mathbf{Z}_0^N), \quad (12)$$

where $\hat{\mathbf{Z}}^i$ and \mathbf{Z}^i are intermediate output and final output at layer i . The MLP consists of two position-wise feed-forward layers and a GELU non-linearity activation function. LN denotes layer normalization, which is applied before every attention block and MLP. The output \mathbf{Z}_0^N of the layer N is also normalized by LN. It is notable that we just apply the fully-connected layer for the final [cls] token, which is further for calculating the expression probability scores. Mathematically, the probability scores are generated as follows:

$$y^i = \frac{e^{\theta_i^T \mathbf{Y}}}{\sum_{i=1}^M e^{\theta_i^T \mathbf{Y}}}, \quad (13)$$

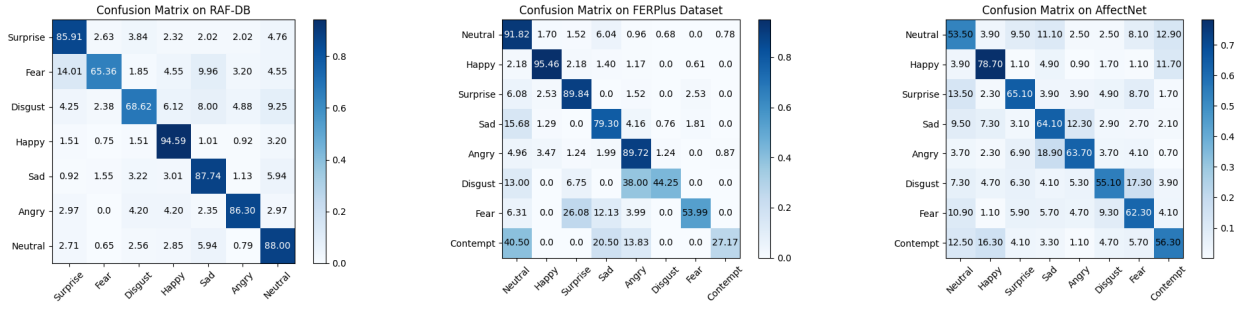
where θ represents the parameters of the fully-connected layer, and the number of expression classes is M . y^i is the probability scores, and the predicted expression category can be easily obtained by arg max function during inference.

4 EXPERIMENTS

To demonstrate the effectiveness of our proposed method, We carry out extensive experiments on three in-the-wild FER datasets (i.e., RAF-DB, FERPlus and AffectNet) and cross-dataset evaluation on CK+. In this section, we first introduce the FER datasets used in our experiments and implementation details. We then compare the proposed method with several state-of-the-art approaches. Subsequently, we explore the impact of each component of CVT on these datasets.

4.1 Datasets

We evaluate our approach on three frequently used facial expression datasets (RAF-DB, FERPlus and AffectNet). These datasets are all collected in the wild, which may suffer from different illuminations and occlusions. To demonstrate the effectiveness of our method when handling occlusion and variant pose issues in real-world conditions, we also conduct experiments on Occlusion-RAF-DB, Pose-RAF-DB, Occlusion-FERPlus, Pose-FERPlus, Occlusion-AffectNet, Pose-AffectNet, which are subsets of



(a) Confusion Matrix of CVT on RAF-DB. (b) Confusion Matrix of CVT on FERPlus. (c) Confusion Matrix of CVT on AffectNet.

Fig. 4. The confusion matrices of our method on RAF-DB, FERPlus and AffectNet.

RAF-DB, FERPlus and AffectNet, respectively. We also conduct cross-dataset evaluation on CK+ to verify the superior generalization ability of our method.

RAF-DB contains 29,672 real-world facial images collected from Flickr. The whole images of RAF-DB are labeled by 315 well-trained annotators and each image is labeled by about 40 independent annotators. The RAF-DB contains two different subsets: single-label subset and multi-label subset. In our experiment, we only use single-label subset, including seven basic emotions (neutral, happiness, surprise, sadness, anger, disgust, fear). The images from single-label subset are split into 12,271 training samples and 3,068 testing samples. The expressions in both training images and test images have imbalanced distribution. The overall sample accuracy is used for performance measurement.

FERPlus is extended from the original FER2013 dataset, which was for the ICML 2013 Challenges in Representation Learning. FERPlus contains 28,709 training images and 3,589 test images, all of which are collected by the Google search engine. The original size of the images in FERPlus is 48×48 . Each image in FERPlus is annotated by 10 annotators, providing better quality labels than the original FER2013 labels. Apart from seven basic emotions as RAF-DB, contempt is included in the labels. We mainly report overall sample accuracy under the supervision of majority voting for performance measurement.

AffectNet is the largest facial expression datasets with more than 1,000,000 facial images collected from the Internet. AffectNet provides both discrete categorical and continuous dimensional (i.e., valence and arousal) annotations. It should be noted that AffectNet has imbalanced training, validation and test sets, of which 450,000 images have been annotated manually. In our experiment, we utilize images annotated with eight basic expressions as FERPlus, 28,7652 images for training, 4,000 images for validating and 4,000 images for testing. Since the test set is not available to the public, we mainly report mean class accuracy on the validation set for performance measurement and fair comparison with other methods.

Occlusion and Pose Variant Datasets, i.e., Occlusion-RAF-DB, Pose-RAF-DB, Occlusion-FERPlus, Pose-FERPlus, Occlusion-AffectNet, Pose-AffectNet are occlusion and pose subsets of RAF-DB, FERPlus, AffectNet respectively and manually collected by [11]. There are various occlusion types occurring in samples of these datasets, such as wear-

ing mask, wearing glasses and objects in upper/bottom face. In addition, variant pose issues can be divided into two categories, poses larger than 30 degrees and poses larger than 45 degrees. The sample distribution can be found in [11]. We report overall sample accuracy or mean class accuracy according to corresponding original datasets.

CK+ is the extended Cohn-Kandade(CK) dataset for facial action unit and expression recognition, collected in a lab-collected environment. The original data of CK+ has 593 video sequences from 123 subjects, 327 of which are annotated with seven basic emotions and contempt. Each of the video sequences consists of images from onset (the first frame) to peak expression (the last frame). We follow previous work to utilize the first frame of a video sequence as a neutral sample and the last frame with the target expression. In total, we obtain 618 images with seven emotions and 654 images with eight emotions for testing. We use the overall sample accuracy to evaluate the generalization capacity of our method.

4.2 Implementation Details

In our experiments, the face images are detected by MTCNN [20] and further resized to the size of 224×224 . For fair comparison with previous state-of-the-art methods, we use the same backbone ResNet18 pre-trained on the MS-Celeb-1M face recognition dataset. The facial features are extracted from the last pooling layer of ResNet18. The learning rate of our methods is initialized as 0.005, and we use a linear learning rate warmup of 1,000 steps and cosine learning rate decay. We use Adam to optimize the whole networks with a batch size of 32 and train the model for 20k steps on RAF and FERPlus, 40k steps on AffectNet, respectively. We implement our method with Pytorch [49] toolbox and conduct all the experiments on a single NVIDIA GTX 1080Ti GPU card.

4.3 Comparison with State-of-the-art Methods

We compare our approach with previous state-of-the-art methods on RAF-DB, FERPlus and AffectNet. We achieve new state-of-the-art results on these datasets to our knowledge. The better performance demonstrates the superiority of our proposed method.

Results on RAF-DB: Comparison with other state-of-the-art methods can be found in Table 1. Methods in [9]

TABLE 1
Comparison with state-of-the-art methods on RAF-DB. The best results are in bold.

method	Year	Angry	Disgust	Fear	Happy	Sad	Surprise	Neutral	Accuracy
VGG [9]	2017	66.05	25.00	37.84	73.08	51.46	53.49	47.21	69.34
baseDCNN [9]	2017	70.99	52.50	50.00	92.91	77.82	79.64	83.09	82.66
Center Loss [9]	2017	68.52	53.13	54.05	93.08	78.45	79.63	83.24	82.86
DLP-CNN [9]	2017	71.60	52.15	62.16	92.83	80.13	81.16	80.29	82.74
FSN [50]	2018	72.80	46.90	56.80	90.50	81.60	81.80	76.90	81.14
gACNN [10]	2018	-	-	-	-	-	-	-	85.07
RAN [11]	2020	-	-	-	-	-	-	-	86.90
SCN [12]	2020	-	-	-	-	-	-	-	87.03
DSAN-VGG-RACE [25]	2020	82.71	56.25	58.11	94.01	83.89	89.06	80.00	85.37
SPWFA-SE [51]	2020	80.00	59.00	59.00	93.00	84.00	88.00	86.00	86.31
Ours	2021	86.03	68.62	65.36	94.59	87.74	85.91	88.00	88.14

TABLE 2
Comparison with state-of-the-art methods on FERPlus and AffectNet.
The best results are in bold.

(a) Results on FERPlus.

Method	Year	Accuracy
CSLD [16]	2016	83.85
ResNet+VGG [52]	2017	87.4
SHCNN [53]	2019	86.54
LDR [54]	2020	87.6
RAN ^o [11]	2020	88.55
RAN [11]	2020	87.85
SCN [12]	2020	88.01
Ours	2021	88.81

(b) Results on AffectNet.

Method	Year	Accuracy
IPA2LT [†] [55]	2018	55.11
gACNN [†] [10]	2018	58.78
SPWFA-SE [†] [51]	2020	59.23
RAN [11]	2020	52.97
RAN* [11]	2020	59.50
SCN* [12]	2020	60.23
Ours*	2021	61.85

present their performance using mean accuracy. For fair comparison, we convert their results to accuracy, following [51]. gACNN [10], RAN [11] and SCN [12] don't report specific expression recognition accuracy or confusion matrices, so the corresponding places are marked with '-'. Although SPWFA-SE [51] also doesn't report specific expression recognition accuracy, it provides the confusion matrix on RAF-DB. Therefore, we borrow accuracy results from its confusion matrix for comparison. Our proposed method achieves 88.14% on RAF-DB. As shown in Table 1, our method achieves all the best results among all methods except for the Surprise category. In detail, our CVT has obtained gains of 18.8% and 1.11% over VGG and SCN, which are the baseline method and the previous SOTA method, respectively. DSAN-VGG-RACE integrates deeply-supervised blocks and attention blocks with race labels, which are additional data compared with our purely used expression labels. Since the RAF-DB also has extremely imbalanced distribution, the slight performance decline of the Surprise category is reasonable and acceptable. The Disgust

recognition accuracy of our method has recorded an increase of 9.62% when compared with the previous best result of [51], which demonstrates the effectiveness and superiority of our method in feature learning.

Results on FERPlus: Table 3(a) presents the comparison on FERPlus. We compare our models with CNN-based methods including CSLD, SHCNN, ResNet+VGG, LDR, as well as two recent state-of-the-art methods(RAN, SCN). As we can see in Tab 3(a), our proposed CVT achieves 88.69% on FERPlus. Under the same experiment settings, total improvements of CVT on FERPlus are 0.84% and 0.68% when compared with RAN and SCN. Especially, RAN^o means original RAN with extra face alignment. Although face alignment is crucial for face recognition and facial expression recognition, it is a preprocessing step and CNN-based methods tend to recognize expression in an end-to-end manner. Even without face alignment in our experiment settings, our CVT also achieves much better results over RAN^o.

Results on AffectNet: We compare our method with several methods on AffectNet and report the results in Table 3(c). We obtain 61.55% with oversampling on AffectNet, without bells and whistles. IPA2LT, gACNN and SPWFA-SE are trained for seven classes on AffectNet without the Contempt category. As mentioned above, AffectNet has imbalanced distribution. SPWFA-SE utilizes focal loss function to handle the imbalance problem. To deal with the imbalance issue, as RAN and SCN do, we adopt the oversampling strategy in our experiments. Our CVT with only AffectNet for training outperforms SCN by 1.32%, which applies extra dataset WebEmotion for pretraining and then finetunes SCN on AffectNet. The improvements of our CVT over previous methods suggest that CVT indeed has better generalization ability even on large-scale expression recognition datasets like AffectNet.

Results on Occlusion and Pose Variant Datasets: To examine our method when facing occlusion and variant pose issues in real scenarios, we also conduct several experiments on Occlusion-RAF-DB, Pose-RAF-DB, Occlusion-FERPlus, Pose-FERPlus, Occlusion-AffectNet and Pose-AffectNet. Table shows the accuracy of the experimental results under corresponding subsets. RAN [11] propose to divide a face image into subregions and use a region biased loss for capturing the importance of different regions for occlusion and pose variant expression recognition. Although our CVT

TABLE 3
Comparison with other methods on Occlusion and Pose Variant Datasets.

(a) Results on Occlusion-RAF-DB, Pose-RAF-DB.			
Method	Occlusion	Pose(30)	Pose(45)
Baseline [11]	80.19	84.04	83.15
RAN [11]	82.72	86.74	85.20
Ours	83.95	87.97	88.35

(b) Results on Occlusion-FERPlus, Pose-FERPlus.			
Method	Occlusion	Pose(30)	Pose(45)
Baseline [11]	73.33	78.11	75.50
RAN [11]	83.63	82.23	80.40
Ours	84.79	88.29	87.20

(c) Results on Occlusion-AffectNet, Pose-AffectNet.			
Method	Occlusion	Pose(30)	Pose(45)
Baseline [11]	49.48	50.10	48.50
RAN [11]	58.50	53.90	53.19
Ours	62.98	60.61	61.00

is not specifically designed for occlusion and variant pose FER issues, our method outperforms RAN with a large margin in each case, which shows the superiority of our method. Specifically, our method exceeds RAN by 1.23%, 1.16% and 4.48% on Occlusion-RAF-DB, Occlusion-FERPlus and Occlusion-AffectNet. Our method also outperforms RAN on Pose-RAF-DB, Pose-FERPlus and Pose-AffectNet. The gains are 1.23%, 6.06% and 6.71% with pose larger than 30 degrees. On Pose-FERPlus, Pose-AffectNet and Pose-RAF-DB with pose larger than 45 degrees, our method significantly outperforms RAN with the gains of 3.15%, 6.8% and 7.81%, respectively. Overall, these results reliably verify the effectiveness of our method on occlusion and variant pose issues.

Results on CK+: We also conduct a cross-dataset evaluation to verify the superior generalization ability of our method. Specifically, We first train the network individually on RAF-DB, FERPlus as well as AffectNet, and then test the model directly on CK+. Table 4 shows that our method achieves better performance comparison with previous approaches. Note that gACNN and SPWFA-SE are trained for predicting seven basic emotions. Although our model predicts one more expression (contempt), which generally lowers down the final results as shown in Fig. 4(b) and Fig. 4(c), the model trained on AffectNet gets an accuracy of 86.54% on CK+. Compared with the gACNN and the SPWFA-SE, our method has better performance and increases by 0.81% and 0.16%. The model trained on AffectNet achieves higher accuracy than the ones trained on RAF-DB and FERPlus, because AffectNet is a relatively large scale dataset and contains more facial images. Table 4 demonstrates that our method has better generalization capacity and achieves better performance without exceptions.

4.4 Ablation Study

As shown in Fig 2, our proposed method CVT consists of LBP features with Attentional Selective Fusion (ASF)

TABLE 4
Cross-dataset evaluation results on CK+.

Method	Train	Test	Accuracy
gACNN [10]	RAF-DB	CK+	81.07
SPWFA-SE [51]	RAF-DB	CK+	81.72
SPWFA-SE [51]	AffectNet	CK+	85.44
Ours	RAF-DB	CK+	81.88
Ours	FERPlus	CK+	83.79
Ours	AffectNet	CK+	86.24

TABLE 5
Ablation study w.r.t. LBP features, ASF and MTE, performed on RAF-DB, FERPlus and AffectNet.

Setting	LBP	ASF	MTE	RAF-DB	FERPlus	AffectNet
a	✗	✗	✗	86.43	86.75	58.41
b	✓	✗	✗	86.62	87.10	58.67
c	✓	✓	✗	87.23	87.48	59.80
d	✗	✗	✓	87.57	87.63	60.48
e	✓	✗	✓	87.84	88.11	60.95
f	✓	✓	✓	88.14	88.69	61.55

and Multi-layer Transformer Encoder (MTE). To validate the generality of these modules, we conduct comparative experiments on RAF, FERPlus and AffectNet by discarding some parts of our CVT, i.e. ASF, MTE, LBP with ASF, ASF and MTE, ASF and MTE, LBP with ASF and MTE. The detail settings of these experiments can be found in Table 5, where the setting a represents the baseline method.

Effectiveness of LBP features for FER. Since our method begins with extracting LBP features, we design the ablation study to investigate the impact of LBP features for FER. Taking results on RAF-DB for example, the baseline on RAF-DB is 86.43 % without any modifications. Adding LBP features improves the baseline by 0.19%. Settings (a, b) and settings (c, d) demonstrate that integrating the LBP features improves the baselines on FERPlus and AffectNet by 0.25% and 0.26%, which also suggests LBP features are beneficial in improving expression recognition performance. This can be explained by that the LBP features can extract texture information and reflect fine facial changes, which show the subtle differences of expressions. Nevertheless, directly using additional LBP features for FER is of limited use, because simple addition fusion strategy is unsatisfactory for combining LBP features and CNN features.

Evaluation of Attentional Selective Fusion (ASF). To verify the effectiveness of ASF for fusing LBP features and CNN features, we conduct experiments by replacing simple element-wise addition with ASF in CVT. According to settings (b, e) and settings (d, f), ASF leads to an increase in recognition accuracy when fusing LBP features and CNN features, showing the effectiveness of the proposed ASF. Specifically, we can see from settings (b, e) that the designed ASF further improves the performance by 0.74%, 0.38% and 1.27%. With additional LBP features, the ASF improves the baseline setting a by 0.8%, 0.94% and 1.41%, respectively. The ASF aggregates global and local contexts for fusing LBP features and CNN features, which further improves the recognition performance.

TABLE 6

Ablation study w.r.t. number of heads, number of layers, performed on RAF-DB, FERPlus and AffectNet. Bold values correspond to better performance.

Setting	N_L	N_H	Params(M)	RAF-DB	FERPlus	AffectNet
i	4	4	51.8	87.45	88.46	61.08
ii	4	8	51.8	88.14	88.69	61.55
iii	4	12	51.8	87.52	88.65	61.85
iv	8	4	80.1	87.22	88.14	60.82
v	8	8	80.1	87.61	88.81	61.23
vi	8	12	80.1	87.48	88.52	61.30
vii	12	4	108.5	87.23	88.20	60.85
viii	12	8	108.5	87.29	88.52	60.45
ix	12	12	108.5	87.09	88.21	61.50

TABLE 7

Comparison between ViT and our CVT.

Setting	N_L	N_H	Params(M)	RAF-DB	FERPlus	AffectNet
ViT	12	12	85.8	47.55	47.72	27.87
ViT*	12	12	85.8	85.14	88.07	58.77
Ours	4	8	51.8	82.27	84.80	58.75
Ours*	4	8	51.8	88.14	88.69	61.55

Effectiveness of Multi-layer Transformer Encoder (MTE). To explore the impact of MTE for our CVT, we evaluate the performance of MTE in this part. We also compare the effects of MTE on RAF-DB, FERPlus and AffectNet. For fair comparison, we constrain the number of heads N_H and the number of layers N_L to 4 and 8, respectively. From settings (a, c), settings (b, d) and settings (e, f), we can clearly see that MTE greatly improves the performance. Specifically, compared with the baseline setting **a**, the setting **c** shows that integrating MTE outperforms the baseline by 1.24%, 0.88% and 2.07% on RAF-DB, FERPlus and AffectNet. The MTE contributes most to the accuracy improvements over the LBP features and ASF. We infer that employing MTE increases the ability of learning discriminative features, outperforming corresponding baselines.

Impact of the number of layers and heads of MTE. Multi-layer Transformer encoder consists of N_L identical layers. The multi-head self-attention in each layer enables the model decomposes the information into N_H representation subspaces and jointly capture discriminative information at different positions. We explore the effects of different layer values N_L and the number of heads N_H from 4 to 12 on RAF-DB, FERPlus and AffectNet. Table 7 compares the performance of different hyperparameter settings of our method in terms of accuracy/mean accuracy and parameters. We observe that increasing the number of layers N_L greatly burdens the parameters of the whole network. Generally, smaller N_L values tend to achieve better recognition performance, and larger N_L values result in excessive parameters at the risk of overfitting. Note that the smaller the value of N_H , the worse performance we may get, because there are not enough subspaces to learn latent representations.

Impact of pre-trained weights. To find out the impact of pre-trained weights on our method, we train our model from scratch and fine-tune it from pre-trained ResNet18



Fig. 5. An illustration of learned attention maps. The first row is raw images, and the second row is attention maps of MTE.

weights. We also give a comparison of ViT and our CVT in Table 7. We implement ViT-Base [46] on these three FER datasets and conduct experiments based on default settings as [46] described. The ViT denotes that it is trained from scratch and ViT* represents we fine-tune it with weights pre-trained on ImageNet-21k and ImageNet. From settings ViT* and Ours*, we can infer that our method achieves better performance but with fewer parameters. The performance of ViT greatly drops when trained from scratch instead of fine-tuning, because the feature extraction capacity of ViT is relatively limited without the guidance of large-scale datasets. The results show that fine-tuning models from pre-trained weights usually results in better performance.

4.5 Visualization

Our method computes relationships between visual words and captures discriminative features for expression recognition. Table 3 provides an empirical evidence to support the effectiveness of our method. To visually demonstrate the superior capacity of our method, we visualize raw images and their corresponding attention weight maps in Fig. 5. We randomly select three occlusion images of RAF-DB, and compute the attention weight maps across all heads. We then recursively multiply the weights of all layers and project them into input image space.

For the first column of Fig. 5, the weight map contains high attention in the bottom, which covers the mouth area. The second column of Fig. 5 shows that our method can identify occlusion regions and highlight discriminative features. Likewise, the raw image of the third column is occluded with a finger on the left part, while our method provides high attention weights on the right part. It is obvious that our method can dynamically model the relationships among visual sentences and highlight discriminative regions to boost recognition performance.

5 CONCLUSION

In this paper, we present Convolutional Visual Transformers (CVT) for facial expression recognition in the wild. The attentional selective fusion in CVT enables the model to dynamically and adaptively combine LBP features and CNN features for improving recognition accuracy. The multi-layer

Transformer encoder utilizes global self-attention mechanism to shift attention to discriminative features from a global perspective. Based on our experiment results, we have observed that the CVT exceeds other state-of-the-art methods on three frequently used facial expression datasets, i.e., RAF-DB, FERPlus, AffectNet.

REFERENCES

- [1] C. Darwin and P. Prodger, *The expression of the emotions in man and animals*. Oxford University Press, USA, 1998. (document)
- [2] Y.-I. Tian, T. Kanade, and J. F. Cohn, "Recognizing action units for facial expression analysis," *IEEE Transactions on Pattern Analysis and Machine Intelligence*, vol. 23, no. 2, pp. 97–115, 2001. (document)
- [3] N. Dalal and B. Triggs, "Histograms of oriented gradients for human detection," in *IEEE Conference on Computer Vision and Pattern Recognition*, vol. 1, 2005, pp. 886–893. (document)
- [4] C. Shan, S. Gong, and P. W. McOwan, "Robust facial expression recognition using local binary patterns," in *IEEE International Conference on Image Processing*, vol. 2, 2005, pp. II–370. (document)
- [5] X. Feng, M. Pietikainen, and A. Hadid, "Facial expression recognition with local binary patterns and linear programming," *Pattern Recognition And Image Analysis C/C of Raspoznavaniye Obrazov I Analiz Izobrazhenii*, vol. 15, no. 2, p. 546, 2005. (document)
- [6] I. Buciu and I. Pitas, "Application of non-negative and local non negative matrix factorization to facial expression recognition," in *Proceedings of the 17th International Conference on Pattern Recognition*, vol. 1, 2004, pp. 288–291. (document)
- [7] S. H. Lee, K. N. Plataniotis, and Y. M. Ro, "Intra-class variation reduction using training expression images for sparse representation based facial expression recognition," *IEEE Transactions on Affective Computing*, vol. 5, no. 3, pp. 340–351, 2014. (document)
- [8] Y. LeCun, B. Boser, J. S. Denker, D. Henderson, R. E. Howard, W. Hubbard, and L. D. Jackel, "Backpropagation applied to handwritten zip code recognition," *Neural Computation*, vol. 1, no. 4, pp. 541–551, 1989. (document)
- [9] S. Li, W. Deng, and J. Du, "Reliable crowdsourcing and deep locality-preserving learning for expression recognition in the wild," in *IEEE Conference on Computer Vision and Pattern Recognition*, 2017, pp. 2584–2593. (document), 2.1, 4.3, 1
- [10] Y. Li, J. Zeng, S. Shan, and X. Chen, "Occlusion aware facial expression recognition using cnn with attention mechanism," *IEEE Transactions on Image Processing*, vol. 28, no. 5, pp. 2439–2450, 2018. (document), 2.1, 1, 2(b), 4.3, 4
- [11] K. Wang, X. Peng, J. Yang, D. Meng, and Y. Qiao, "Region attention networks for pose and occlusion robust facial expression recognition," *IEEE Transactions on Image Processing*, vol. 29, pp. 4057–4069, 2020. (document), 2.1, 4.1, 1, 2(a), 2(b), 4.3, 4.3, 3(a), 3(b), 3(c)
- [12] K. Wang, X. Peng, J. Yang, S. Lu, and Y. Qiao, "Suppressing uncertainties for large-scale facial expression recognition," in *Proceedings of the IEEE Conference on Computer Vision and Pattern Recognition*, 2020, pp. 6897–6906. (document), 2.1, 1, 2(a), 2(b), 4.3
- [13] P. Lucey, J. F. Cohn, T. Kanade, J. Saragih, Z. Ambadar, and I. Matthews, "The extended cohn-kanade dataset (ck+): A complete dataset for action unit and emotion-specified expression," in *IEEE Conference on Computer Vision and Pattern Recognition-workshops*, 2010, pp. 94–101. (document)
- [14] M. Valstar and M. Pantic, "Induced disgust, happiness and surprise: an addition to the mmi facial expression database," in *Proc. 3rd Intern. Workshop on EMOTION (satellite of LREC): Corpora for Research on Emotion and Affect*, 2010, p. 65. (document)
- [15] G. Zhao, X. Huang, M. Taini, S. Z. Li, and M. Pietikäinen, "Facial expression recognition from near-infrared videos," *Image and Vision Computing*, vol. 29, no. 9, pp. 607–619, 2011. (document)
- [16] E. Barsoum, C. Zhang, C. C. Ferrer, and Z. Zhang, "Training deep networks for facial expression recognition with crowd-sourced label distribution," in *Proceedings of the 18th ACM International Conference on Multimodal Interaction*, 2016, pp. 279–283. (document), 2(a)
- [17] A. Mollahosseini, B. Hasani, and M. H. Mahoor, "Affectnet: A database for facial expression, valence, and arousal computing in the wild," *IEEE Transactions on Affective Computing*, vol. 10, no. 1, pp. 18–31, 2017. (document)
- [18] S. Li and W. Deng, "Deep facial expression recognition: A survey," *IEEE Transactions on Affective Computing*, 2020. (document)
- [19] W. Zheng, H. Tang, T. S. Huang, A. Konar, and A. Charkraborty, "Emotion recognition from non-frontal facial images," *Emotion Recognition: A Pattern Analysis Approach*, vol. 1, pp. 183–213, 2014. (document)
- [20] K. Zhang, Z. Zhang, Z. Li, and Y. Qiao, "Joint face detection and alignment using multitask cascaded convolutional networks," *IEEE Signal Processing Letters*, vol. 23, no. 10, pp. 1499–1503, 2016. (document), 4.2
- [21] B. Amos, B. Ludwiczuk, M. Satyanarayanan *et al.*, "Openface: A general-purpose face recognition library with mobile applications," *CMU School of Computer Science*, vol. 6, no. 2, 2016. (document)
- [22] F. Bourel, C. C. Chibelushi, and A. A. Low, "Recognition of facial expressions in the presence of occlusion," in *Proceedings of the British Machine Vision Conference*, 2001, pp. 1–10. (document)
- [23] S. Happy and A. Routray, "Automatic facial expression recognition using features of salient facial patches," *IEEE Transactions on Affective Computing*, vol. 6, no. 1, pp. 1–12, 2014. (document)
- [24] Y. Li, J. Zeng, S. Shan, and X. Chen, "Patch-gated cnn for occlusion-aware facial expression recognition," in *24th International Conference on Pattern Recognition*, 2018, pp. 2209–2214. (document)
- [25] Y. Fan, V. Li, and J. C. Lam, "Facial expression recognition with deeply-supervised attention network," *IEEE Transactions on Affective Computing*, 2020. (document), 2.1, 1
- [26] J. Li, K. Jin, D. Zhou, N. Kubota, and Z. Ju, "Attention mechanism-based cnn for facial expression recognition," *Neurocomputing*, vol. 411, pp. 340–350, 2020. (document), 2.2
- [27] N. Sun, Q. Lu, W. Zheng, J. Liu, and G. Han, "Unsupervised cross-view facial expression image generation and recognition," *IEEE Transactions on Affective Computing*, 2020. (document)
- [28] W. Zheng, Y. Zong, X. Zhou, and M. Xin, "Cross-domain color facial expression recognition using transductive transfer subspace learning," *IEEE Transactions on Affective Computing*, vol. 9, no. 1, pp. 21–37, 2016. (document)
- [29] K. He, X. Zhang, S. Ren, and J. Sun, "Deep residual learning for image recognition," in *Proceedings of the IEEE Conference on Computer Vision and Pattern Recognition*, 2016, pp. 770–778. 2.1, 3.1
- [30] G. Huang, Z. Liu, L. Van Der Maaten, and K. Q. Weinberger, "Densely connected convolutional networks," in *Proceedings of the IEEE Conference on Computer Vision and Pattern Recognition*, 2017, pp. 4700–4708. 2.1
- [31] Y. Tang, "Deep learning using linear support vector machines," *arXiv preprint arXiv:1306.0239*, 2013. 2.1
- [32] T. Xu, J. White, S. Kalkan, and H. Gunes, "Investigating bias and fairness in facial expression recognition," in *European Conference on Computer Vision*, 2020, pp. 506–523. 2.1
- [33] K.-H. Pong and K.-M. Lam, "Multi-resolution feature fusion for face recognition," *Pattern Recognition*, vol. 47, no. 2, pp. 556–567, 2014. 2.2
- [34] T.-Y. Lin, P. Dollár, R. Girshick, K. He, B. Hariharan, and S. Belongie, "Feature pyramid networks for object detection," in *Proceedings of the IEEE Conference on Computer Vision and Pattern Recognition*, 2017, pp. 2117–2125. 2.2
- [35] G. Lin, A. Milan, C. Shen, and I. Reid, "Refinenet: Multi-path refinement networks for high-resolution semantic segmentation," in *Proceedings of the IEEE Conference on Computer Vision and Pattern Recognition*, 2017, pp. 1925–1934. 2.2
- [36] Y. Hu, Z. Zeng, L. Yin, X. Wei, X. Zhou, and T. S. Huang, "Multi-view facial expression recognition," in *2008 8th IEEE International Conference on Automatic Face & Gesture Recognition*, 2008, pp. 1–6. 2.2
- [37] S. Moore and R. Bowden, "Local binary patterns for multi-view facial expression recognition," *Computer Vision and Image Understanding*, vol. 115, no. 4, pp. 541–558, 2011. 2.2
- [38] J. Chen, Z. Chen, Z. Chi, and H. Fu, "Facial expression recognition in video with multiple feature fusion," *IEEE Transactions on Affective Computing*, vol. 9, no. 1, pp. 38–50, 2016. 2.2
- [39] J. Shao and Y. Qian, "Three convolutional neural network models for facial expression recognition in the wild," *Neurocomputing*, vol. 355, pp. 82–92, 2019. 2.2
- [40] A. Vaswani, N. Shazeer, N. Parmar, J. Uszkoreit, L. Jones, A. N. Gomez, L. Kaiser, and I. Polosukhin, "Attention is all you need," *arXiv preprint arXiv:1706.03762*, 2017. 2.3, 3.1
- [41] J. Beal, E. Kim, E. Tzeng, D. H. Park, A. Zhai, and D. Kislyuk, "Toward transformer-based object detection," *arXiv preprint arXiv:2012.09958*, 2020. 2.3

- [42] S. Yang, Z. Quan, M. Nie, and W. Yang, "Transpose: Towards explainable human pose estimation by transformer," *arXiv preprint arXiv:2012.14214*, 2020. 2.3
- [43] P. Esser, R. Rombach, and B. Ommer, "Taming transformers for high-resolution image synthesis," *arXiv preprint arXiv:2012.09841*, 2020. 2.3
- [44] Y. Wang, Z. Xu, X. Wang, C. Shen, B. Cheng, H. Shen, and H. Xia, "End-to-end video instance segmentation with transformers," *arXiv preprint arXiv:2011.14503*, 2020. 2.3
- [45] M. Bhat, J. Francis, and J. Oh, "Trajformer: Trajectory prediction with local self-attentive contexts for autonomous driving," *arXiv preprint arXiv:2011.14910*, 2020. 2.3
- [46] A. Dosovitskiy, L. Beyer, A. Kolesnikov, D. Weissenborn, X. Zhai, T. Unterthiner, M. Dehghani, M. Minderer, G. Heigold, S. Gelly *et al.*, "An image is worth 16x16 words: Transformers for image recognition at scale," *arXiv preprint arXiv:2010.11929*, 2020. 2.3, 3.1, 3.3, 4.4
- [47] J. Deng, W. Dong, R. Socher, L.-J. Li, K. Li, and L. Fei-Fei, "Imagenet: A large-scale hierarchical image database," in *IEEE Conference on Computer Vision and Pattern Recognition*, 2009, pp. 248–255. 2.3
- [48] W. Wang, E. Xie, X. Li, D.-P. Fan, K. Song, D. Liang, T. Lu, P. Luo, and L. Shao, "Pyramid vision transformer: A versatile backbone for dense prediction without convolutions," *arXiv preprint arXiv:2102.12122*, 2021. 2.3
- [49] A. Paszke, S. Gross, F. Massa, A. Lerer, J. Bradbury, G. Chanan, T. Killeen, Z. Lin, N. Gimelshein, L. Antiga *et al.*, "Pytorch: An imperative style, high-performance deep learning library," *arXiv preprint arXiv:1912.01703*, 2019. 4.2
- [50] S. Zhao, H. Cai, H. Liu, J. Zhang, and S. Chen, "Feature selection mechanism in cnns for facial expression recognition." in *Proceedings of the British Machine Vision Conference*, 2018, p. 317. 1
- [51] Y. Li, G. Lu, J. Li, Z. Zhang, and D. Zhang, "Facial expression recognition in the wild using multi-level features and attention mechanisms," *IEEE Transactions on Affective Computing*, 2020. 1, 2(b), 4.3, 4
- [52] C. Huang, "Combining convolutional neural networks for emotion recognition," in *IEEE MIT Undergraduate Research Technology Conference (URTC)*, 2017, pp. 1–4. 2(a)
- [53] S. Miao, H. Xu, Z. Han, and Y. Zhu, "Recognizing facial expressions using a shallow convolutional neural network," *IEEE Access*, vol. 7, pp. 78 000–78 011, 2019. 2(a)
- [54] X. Fan, Z. Deng, K. Wang, X. Peng, and Y. Qiao, "Learning discriminative representation for facial expression recognition from uncertainties," in *2020 IEEE International Conference on Image Processing*, 2020, pp. 903–907. 2(a)
- [55] J. Zeng, S. Shan, and X. Chen, "Facial expression recognition with inconsistently annotated datasets," in *Proceedings of the European Conference on Computer Vision*, 2018, pp. 222–237. 2(b)